EXTENSION OF A NUMERICAL SOLUTION FOR THE AERODYNAMIC CHARACTERISTICS OF A WING TO INCLUDE A CANARD OR HORIZONTAL TAIL

By Barrett L. Shrout
Langley Research Center
National Aeronautics and Space Administration
Hampton, Virginia

SUMMARY

A method for predicting the aerodynamic lifting surface characteristics of wing-horizontal tail configurations or canard wing configurations at supersonic speeds is discussed. The numerical solution has been programed for a digital computer and is part of a complex of computer programs used in the design, optimization, and evaluation of aircraft configurations at supersonic speeds. The method is an extension of the Carlson-Middleton numerical solution for lifting surfaces, which is briefly reviewed. The present method predicts lift, drag, and moment characteristics over a range of lift coefficients and for various control settings. Theoretical and experimental data are compared for wing-horizontal tail configurations and for canard-wing configurations at various Mach numbers. These comparisons show both the basic data with control deflections and some final trimmed drag polars. Some data are also presented to show the extent to which program limitations affect the accuracy of the analytic methods.

SYMBOLS

$A(L, N)$	weighting factor for partial grid elements
$\bar{c}$	mean geometric chord
C_D	drag coefficient, D/qS
C_L	lift coefficient, L/qS
C_m	pitching-moment coefficient, $M'/qS\bar{c}$
Cm_o	pitching-moment coefficient at zero lift
ΔCm_o	increment in Cm_o for control deflection
$\Delta Cm/\Delta C_L$	stability level, measured in the vicinity of zero lift
ΔC_p	lifting pressure coefficient
D	drag
L	lift
L, N	coordinates of influencing grid elements
L^*, N^*	coordinates of field-point grid element
M	free-stream Mach number
M'	pitching moment
q	dynamic pressure
$\bar{R}$	grid element influence function
S	wing reference area
w	downwash strength
x, y, z	Cartesian coordinate system, x-axis streamwise
z_c	camber surface ordinate
α	angle of attack
$\beta = \sqrt{M^2-1}$	
δ_H	horizontal tail deflection, positive trailing edge down
δ_C	canard deflection, positive trailing edge down
δ_F	flap or elevon deflection, positive trailing edge down

Subscripts:

W	wing
B	body plus vertical tail
T	horizontal tail

EXTENSION OF A NUMERICAL SOLUTION FOR THE AERODYNAMIC CHARACTERISTICS OF A WING TO INCLUDE A CANARD OR HORIZONTAL TAIL

By Barrett L. Shrout
NASA Langley Research Center
Hampton, Virginia

INTRODUCTION

With the arrival of the supersonic jet era, the aerodynamicist has realized that the characteristics of a configuration can no longer be considered the sum of the characteristics of its component parts. Mutual aerodynamic interference between components has a significant effect on the overall aerodynamic characteristics of a configuration; as a consequence, extensive wind-tunnel testing must be done for configuration design and analysis. As an alternative, the aerodynamicist can use analytic techniques for much of the preliminary design and evaluation work with wind-tunnel testing used for final verification.

NASA's Langley Research Center has been working in recent years toward the development of a systematic method of analysis for supersonic configurations utilizing high-speed digital computers. From this effort has evolved a complex of computer programs used to estimate wave drag, skin-friction drag, and drag-due-to-lift of supersonic aircraft configurations. Until recently, it has been necessary to estimate stability and control characteristics using empirical techniques, or to obtain them from wind-tunnel data.

The method and results of modifying the lifting-surface analysis program to predict stability and control characteristics for tailless, wing-horizontal tail, and canard-wing configurations are presented in this paper. The experimental data presented were taken primarily from references (7) through (15).

DISCUSSION

A block diagram illustrating the Langley supersonic analysis computer program complex is shown in figure 1. In brief, the configuration to be analyzed is reduced to a numerical model in which all wing coordinates, thickness ratios, camber lines, body contours, empennage, and so forth, are expressed in x, y, and z coordinates, as a computer card deck. This numerical model, or components of it, is then input to the selected computer program and the desired component of drag is calculated.

An illustration of a typical numerical model is shown in figure 2. The complexity of the numerical model and the attention to detail in the description of the configuration are obvious in this drawing. The drawing, which is machine plotted from a tape made using the numerical model as input, serves a very useful function in that it provides a check on the accuracy of the numerical model. Misplaced decimals or incorrect numbers become quite obvious in these drawings, which may be three-view, oblique, or perspective.

The three principle programs required to establish a basic drag polar are the skin-friction drag program, the wave drag program, and the drag-due-to-lift program. A typical drag polar, illustrating the use of these three programs is shown in figure 3. The wave drag program calculates the drag due to volume at zero lift using the method of reference (1). The method utilizes a far-field approach by relating the drag to the momentum flow outward through a large cylindrical control surface whose longitudinal axis is the flight path. Skin friction is evaluated by the Sommer and Short T' method of reference (2) with the skin friction of each component calculated and then summed. The drag-due-to-lift calculation utilizes the Carlson-Middleton method of reference (3) and uses a near-field method whereby differential pressures are calculated over the mean camber plane of the configuration.

The sum of these drag components yields the basic drag polar. Performance analysis, however, requires a drag polar for the configuration in a trimmed condition. Until recently, it has been necessary to obtain pitching-moment curves and control increments from wind-tunnel data in order to establish trimmed drag polars. The drag-due-to-lift program has been modified to provide control increments for tailless configurations and to provide stability levels and control increments for wing-horizontal tail configuration and for canard-wing configurations.

The method utilized in the drag-due-to-lift program is illustrated in figure 4. The mean camber plane is represented in the program by a grid element system, each block of which is inclined to the flow at an angle determined by the camber plane in that region. For an uncambered wing, the inclination angles are all zero.

Consider a pair of elements in the grid system. The forward element (coordinates L, N) generates a downwash w which affects all the elements in the trailing Mach cone. The differential pressure ΔC_p at the field point L^*, N^* is calculated from the influence of the element L, N (and all other elements in the fore Mach cone from the field point) using the equation shown. The term $\partial z_c/\partial x$ is the slope of the camber surface at the field point. The term A(L, N) is a weighting factor for grid element size allowing partial grid elements to be used along the leading and trailing edges. The term $\bar{K}$ is an influence function indicating the field point position in the downwash of the preceding elements. The calculation process begins at the apex and proceeds across each grid element row while proceeding toward the trailing edge. Thus the differential pressure of each element in the fore Mach cone of each field point has previously been calculated. Simultaneously, calculations are made for the planform as a flat plate at 1° angle of attack. Once the differential pressures over the surface are known, they are integrated to provide force and moment coefficients. A superposition technique using the flat plate and cambered wing data provides for the variation of drag with lift.

A more detailed explanation of the numerical solution can be found in references (3) and (4).

The modifications made to the program to account for a horizontal tail are shown in figure 5. The wing and forebody are handled in a manner much the same as the original program. The afterbody and horizontal tail have been added and the grid system extended as shown on the right side of the sketch. The region outboard of the body, aft of the wing trailing edge, and forward of the tail leading edge is a region of zero loading; that is, there is no surface within this region to support a pressure differential. Grid elements on the tail are still influenced by the part of the wing within their fore Mach cones, and these wing pressures are included in the calculation of the tail pressure distributions.

Some of the general characteristics of the lifting surface programs are listed on figure 5. The mean camber plane input to the program may be cambered and twisted or a flat plate. The forebody may be cambered and the wing planform is arbitrary. For the horizontal-tail program specifically, the tail may be of arbitrary planform and control inputs may be for either a full slab tail deflection or deflection of elevators on the tail.

It should be noted that the program is relatively easy to use. Inputs consist primarily of leading and trailing edge coordinates for the wing-body and horizontal tail, and streamwise camber lines composed of z coordinates at specified percent chord stations. The grid system is imposed within the program and an interpolation routine assigns a suitable deflection to each grid element. The grid system shown on the slide is only a crude representation; in actual practice, depending on Mach number, a system 30 to 40 elements for the semispan and 90 to 100 elements in length is utilized. Computation time for a single Mach number and control deflection takes approximately 3 minutes on a CDC 6600 series computer, using 70 000 octal storage.

Figure 6 shows a comparison between experimental force and moment coefficients and estimates made using the horizontal tail program. The configuration is a delta wing configuration with a rather close-coupled horizontal tail. At a Mach number of 1.5 the agreement between theory and experiment is excellent. No attempt was made to calculate the minimum drag level for any of the configurations in this paper, rather the experimental drag value at zero lift for undeflected controls was added to the estimated drag-due-to-lift values. Drag increments due to control deflections, drag at lift, and the pitching-moment data are plotted directly from the program output. The data for a Mach number of 2.5 are more typical of the program estimates when compared with experiment, in that the drag-due-to-lift is slightly underpredicted, and the stability level slightly overpredicted. In general, these discrepancies can be attributed to the limitations of linear theory, the assumptions of small angles and completely attached flow.

The overprediction of stability level and the underprediction of drag-due-to-lift are compensating factors when a trim drag polar is calculated in that the theoretical data trims at a lower C_L for a given tail deflection but at a lower drag level. The theoretical trim drag polar is shown by the heavy line and the experimental trim points by the solid symbols.

Figure 7 shows estimated and experimental data for another horizontal tail configuration. In this example, the configuration has an arrow wing and the separation between wing and horizontal tail is somewhat greater than for the previous configuration. The stability levels again are somewhat overpredicted and the drag-due-to-lift slightly underpredicted. In the case of the data for Mach number 1.41, the Cm_o increments are overpredicted by about 25 percent. Whether this disparity in Cm_o is peculiar to this configuration or is generally true for configurations with large separations of wing and horizontal tail will require further investigation.

As mentioned earlier, the basic lifting surface program was also modified to handle a canard-wing configuration. Figure 8 shows in schematic how this is accomplished. The method is much the same as that used for the inclusion of a horizontal tail except that,for this case, the control surface is ahead of the wing and the region of zero loading is outboard of the body, aft of the canard trailing edge, and forward of the wing leading edge. Note that as for all the programs in this series, partial grid elements are used to better define the leading and trailing edges of all surfaces. In addition to the features of the other programs, this program allows for an arbitrary planform canard, but is restricted to deflections of the entire canard surface; that is, the provision for deflecting a trailing-edge canard flap is not included at the present time.

Figure 9 shows a comparison between theory and experiment for a delta wing configuration with a canard control surface. At a Mach number of 1.41, the zero lift-drag increments and increments in Cm_o due to control deflection are predicted quite well. The stability levels are again slightly overpredicted. The drag-due-to-lift variation is accurately estimated with the exception of the data for the 15° canard deflection. In this case it appears that the experimental value is unexplainably low. In general, between 10° and 15° control setting, a sizable experimental drag increment occurs at all lift coefficients. In this case, for the higher lift coefficients, the experimental drag increment is of the same order as the increment between smaller control deflections. At the higher Mach number, the correlation is much the same; however, the drag increment for the maximum canard deflection is in better agreement than it was at the lower Mach number.

Data for a second canard configuration are shown on figure 10. The configuration is identical to the previous configuration, except that it has a trapezoidal wing. The correlation between theory and experiment is quite good. The stability level is overpredicted by about 4 percent $\bar{c}$ at the lower Mach number and by about 2 percent $\bar{c}$ at the high Mach number. Drag-due-to-lift is slightly underpredicted at the lower Mach number, and the increment in Cm_o for the maximum control deflection is slightly overpredicted at both Mach numbers. Because the other Cm_o increments are predicted so well, this indicates that the variation of C_m with canard deflection angle has become nonlinear between 10° and 15° and, of course, the theoretical method used herein does not account for such nonlinearities.

Figure 11 shows a correlation between experiment and theory of the stability and control parameters for the two programs shown thus far. The data cover several configurations in addition to the ones which have been presented in this paper. The circular symbols are for horizontal tail configurations; the square symbols represent canard configurations. The solid line represents perfect agreement between theory and

experiment. The Cm_o increments show generally good agreement; for the most part, the estimated values are between zero and 15 percent high. For the stability parameter, $\Delta C_m/\Delta C_L$, the data fall on either side of the line of perfect agreement; for a majority of cases the stability parameter is slightly overpredicted. Examination of the data for both parameters revealed no particular pattern related to Mach number. The canard configurations generally appear to correlate better; however there were fewer of these configurations examined and thus no conclusions are drawn as to the relative merits of the two programs.

The theoretical method of this paper assumes a planar system, that is, all the grid elements lie in a constant z plane. To indicate the magnitude of error that occurs when the configuration does not satisfy this assumption, data are shown in figure 12 for a configuration with a horizontal tail located above or below the wing plane.

The upper part of the figure shows the experimental data for the two tail positions at two Mach numbers. The present method which, of course,yields a single curve, is shown by a solid line. For comparison, a prediction made using the Nielsen-Kaattari method (ref. (5)), which is also a planar method, is shown. The bottom part of the figure shows the data as a function of angle of attack, with the body-tail moment contribution subtracted out so that the remaining increment is the wing contribution plus the effect of the wing on the horizontal tail. It appears that the principle effect of tail location on Cm_o, for this configuration, is the relation of the tail to the body, rather than the relation of the tail to the wing. Regardless of the cause for the Cm_o change, the present method does not account for it, and as can be seen from the basic data at the top of the figure, the effect can be rather significant. Thus, further study is indicated in this area.

Finally, an attempt was made to modify the basic program to calculate control characteristics for tailless configurations. This merely consisted of assigning the desired control deflection to all grid elements which fall within the flap or elevon planform. A correlation for two configurations with trailing-edge controls is shown on figure 13. The configuration on the left has trailing-edge controls over approximately 70 percent of the span. For the configuration on the right, the controls extend approximately 30 percent of the span. The drag-due-to-lift estimate for both configurations is considerably lower than the experimental data. This was unexpected because, for zero control deflection, the modified program is the same as the basic program which generally gives much better estimates. The increment in Cm_o for the configuration with the wide span flaps is somewhat overpredicted. This difference between theory and experiment can be related to the results of reference (6), where it was shown that controls in the vicinity of the wing tip, operating in a region where aeroelastic deformation and flow separation can occur, yielded experimental increments only 70 percent of the estimated increments. For the configuration with the short span controls, the drag and moment increments for the 10° deflection are good; for the 20° deflection, only fair. The stability levels for both configurations are slightly overpredicted.

CONCLUDING REMARKS

A method has been discussed in which the Carlson-Middleton numerical solution for lifting surfaces can be extended to include a horizontal tail or canard. In general, the method slightly overpredicts stability levels, and predicts relatively well drag increments and increments in Cm_o due to control deflections. The solution is for a planar system, and significant errors may be introduced in the predicted data if the control surface is well out of the wing plane.

REFERENCES

(1) Harris, Roy V., Jr.:
An Analysis and Correlation of Aircraft Wave Drag
NASA TM X-947 (1964)

(2) Sommer, Simon C.; and Short, Barbara J.:
Free-Flight Measurements of Turbulent-Boundary-Layer Skin Friction in the Presence of Severe Aerodynamic Heating at Mach Numbers From 2.8 to 7.0
NACA TN D-3391 (1955)

(3) Middleton, Wilbur D.; and Carlson, Harry W.:
A Numerical Method for Calculating the Flat-Plate Pressure Distributions on Supersonic Wings of Arbitrary Planform
NASA TN D-2570 (1965)

(4) Carlson, Harry W.; and Middleton, Wilbur D.:
A Numerical Method for the Design of Camber Surfaces of Supersonic Wings With Arbitrary Planforms
NASA TN D-2341 (1964)

(5) Nielsen, Jack N.; Kaattari, George E.; and Anastasio, Robert F.:
A Method for Calculating the Lift and Center of Pressure of Wing-Body-Tail Combinations at Subsonic, Transonic, and Supersonic Speeds
NACA RM A53G08 (1953)

(6) Landrum, Emma Jean:
Effect of Skewed Wing-Tip Controls on a Highly-Swept Arrow Wing at Mach Number 2.03
NASA TN D-1867 (1964)

(7) Smith, Norman F.; and Hasel, Lowell E.:
An Investigation at Mach Numbers of 1.41 and 2.01 of Aerodynamic Characteristics of a Swept-Wing Supersonic Bomber Configuration
NACA RM L52J17 (1952)

(8) Driver, Cornelius:
Longitudinal and Lateral Stability and Control Characteristics of Two Canard Airplane Configurations at Mach Numbers of 1.41 and 2.01
NACA RM L56L19 (1957)

(9) Spearman, M. Leroy; and Driver, Cornelius:
Longitudinal and Lateral Stability and Control Characteristics at Mach Number 2.01 of a 60° Delta-Wing Airplane Configuration Equipped With a Canard Control and With Wing-Trailing-Edge Flaps
NACA RM L58A20 (1958)

(10) Hilton, John H., Jr.; and Palazzo, Edward B.:
Wind Tunnel Investigation of a Modified 1/20-Scale Model of the Convair MX-1554 Airplane at Mach Numbers of 1.41 and 2.01
NACA RM SL 53G30 (1953)

(11) Driver, Cornelius; and Foster, Gerald V.:
Static Longitudinal Stability and Control Characteristics of a Model of a 45° Swept Wing Fighter Airplane at Mach Numbers of 1.41, 1.61, and 2.01
NACA RM L56D04 (1956)

(12) Church, James D.:
Effects of Components and Various Modifications on the Drag and the Static Stability and Control Characteristics of a 42° Swept-Wing Fighter-Airplane Model at Mach Numbers of 1.60 to 2.50
NACA RM L57K01 (1957)

(13) Spearman, M. Leroy:
Static Longitudinal Stability and Control Characteristics of a 1/16-Scale Model of the Douglas D-558-II Research Airplane at Mach Numbers of 1.61 and 2.01
NACA RM L53I22 (1953)

(14) Spearman, M. Leroy; and Driver, Cornelius:
Effects of Canard Surface Size on Stability and Control Characteristics of Two Canard Airplane Configurations at Mach Numbers of 1.41 and 2.01
NACA RM L57L17a (1958)

(15) Foster, Gerald V.:
Investigation of the Longitudinal Aerodynamic Characteristics of a Trapezoidal-Wing Airplane Model With Various Vertical Positions of the Wing and Horizontal Tail at Mach Numbers of 1.41 and 2.01
NACA RM L58A07 (1957)

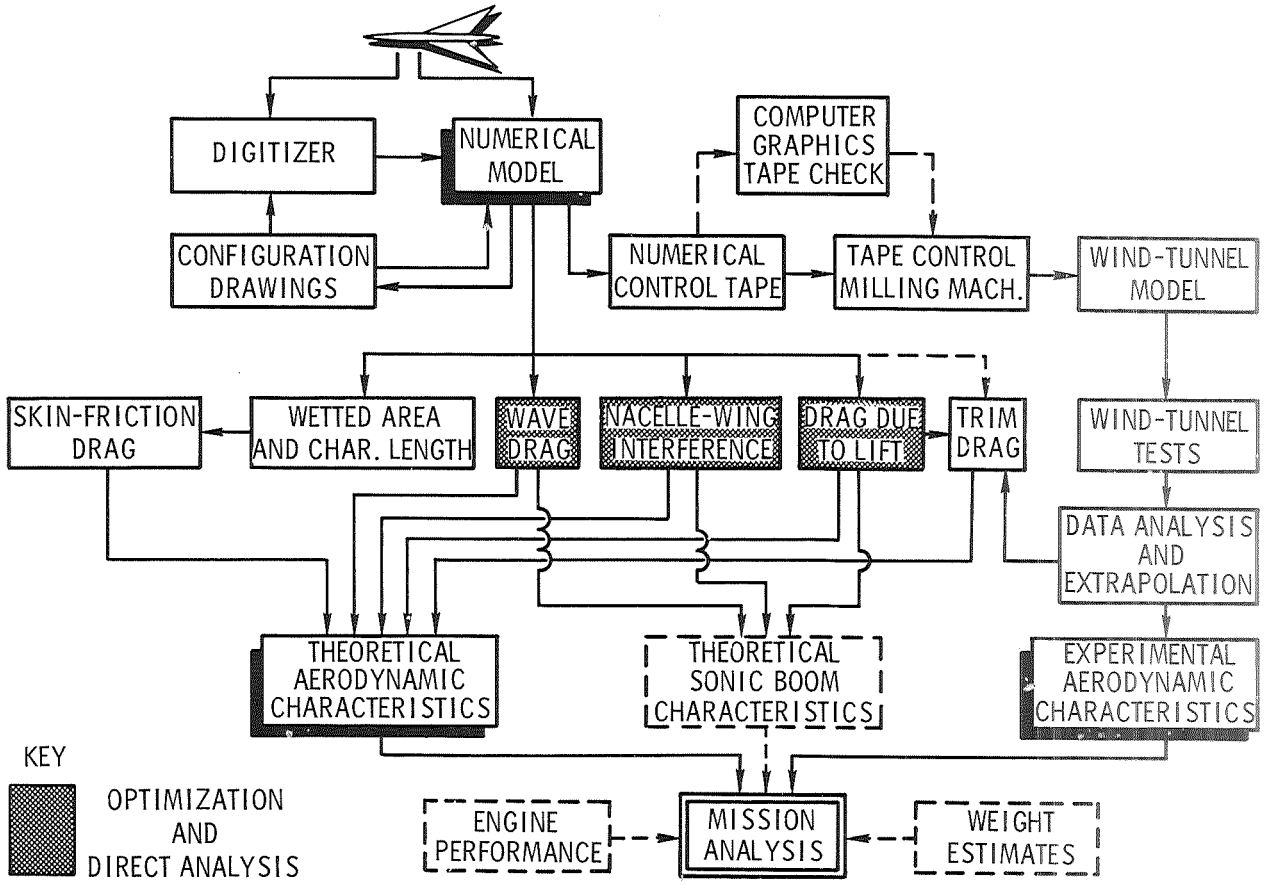

Figure 1. Complex of computer programs for supersonic aircraft design and evaluation.

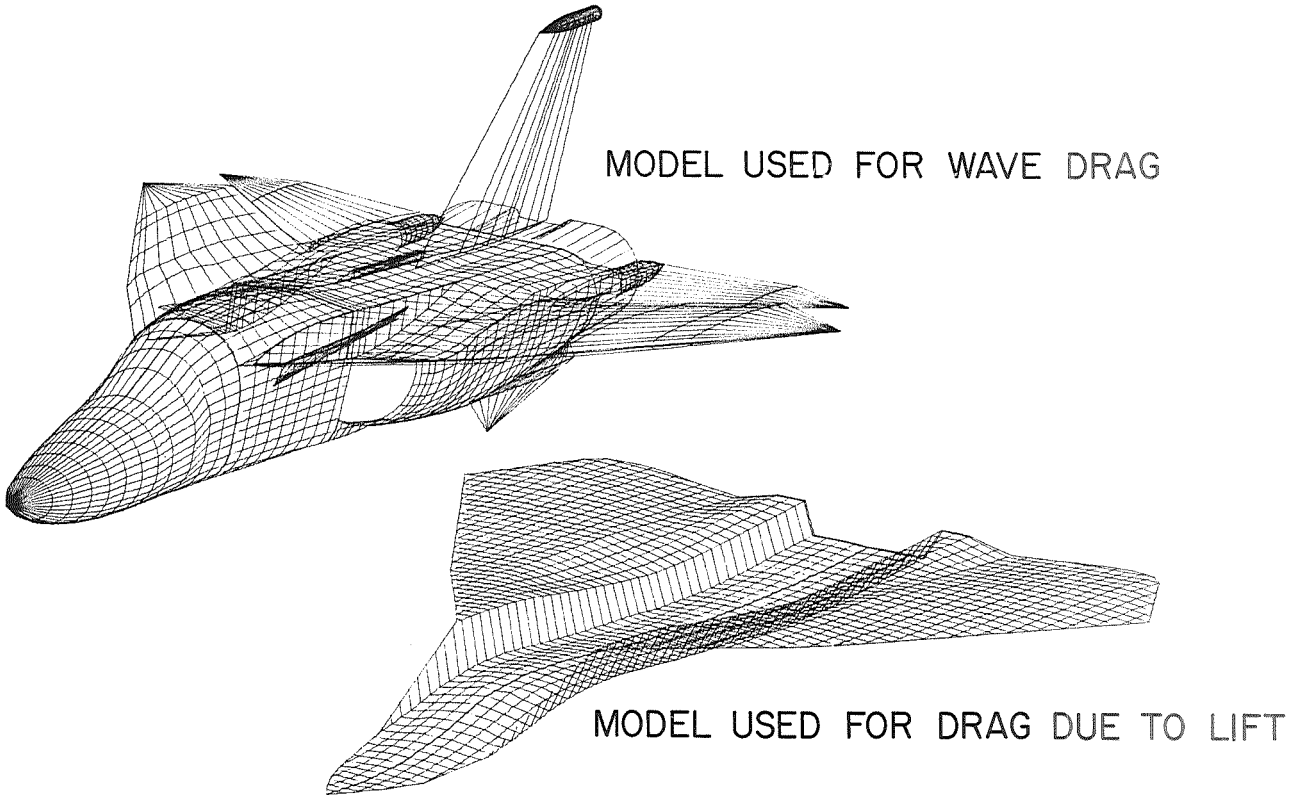

Figure 2. Computer drawings of numerical models.

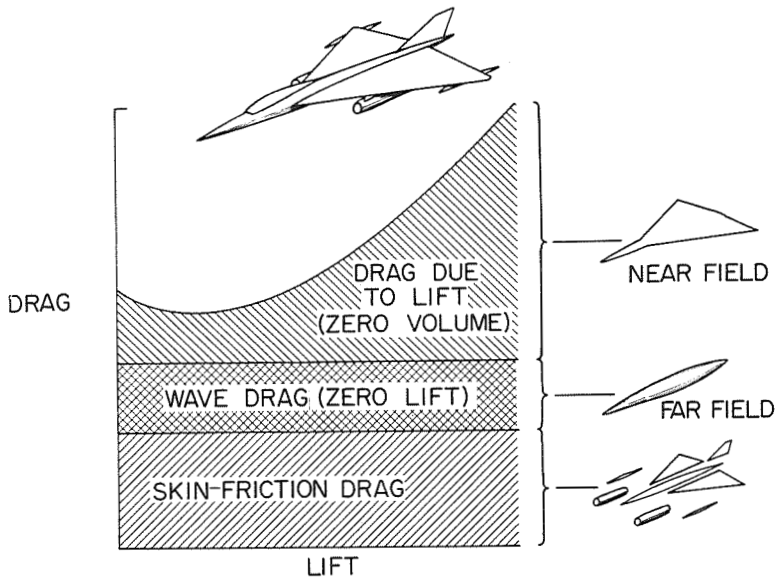

Figure 3. A composite system of supersonic drag analysis.

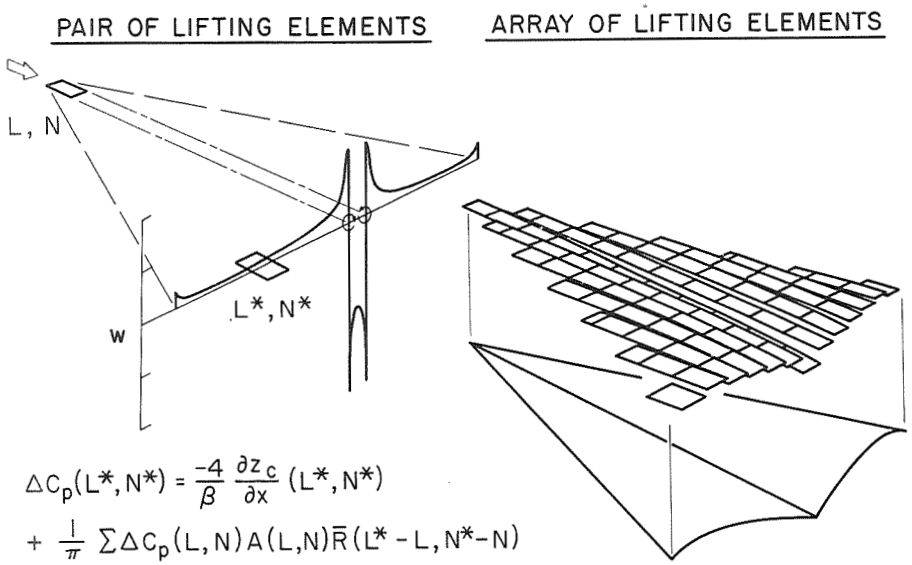

Figure 4. Lifting-surface representation.

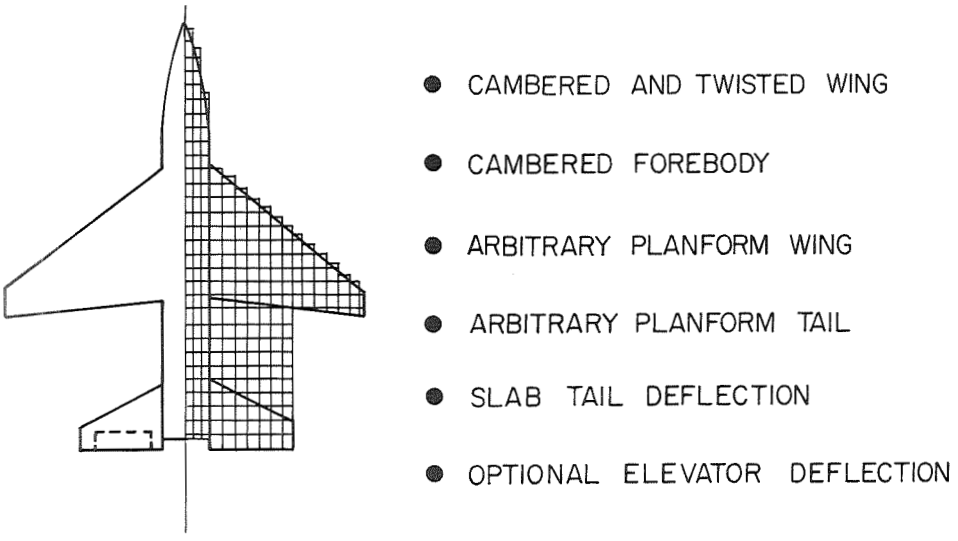

Figure 5. Wing horizontal-tail configuration.

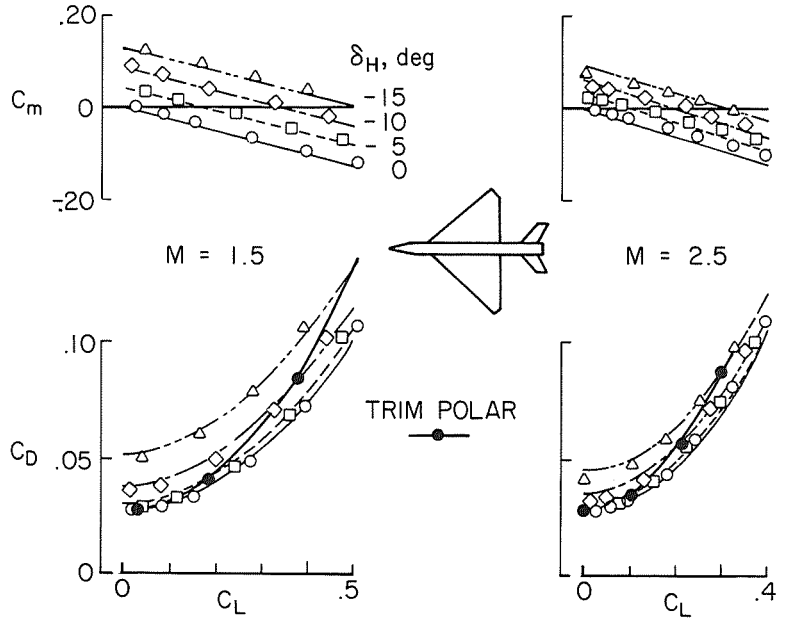

Figure 6. Delta-wing configuration with horizontal tail.

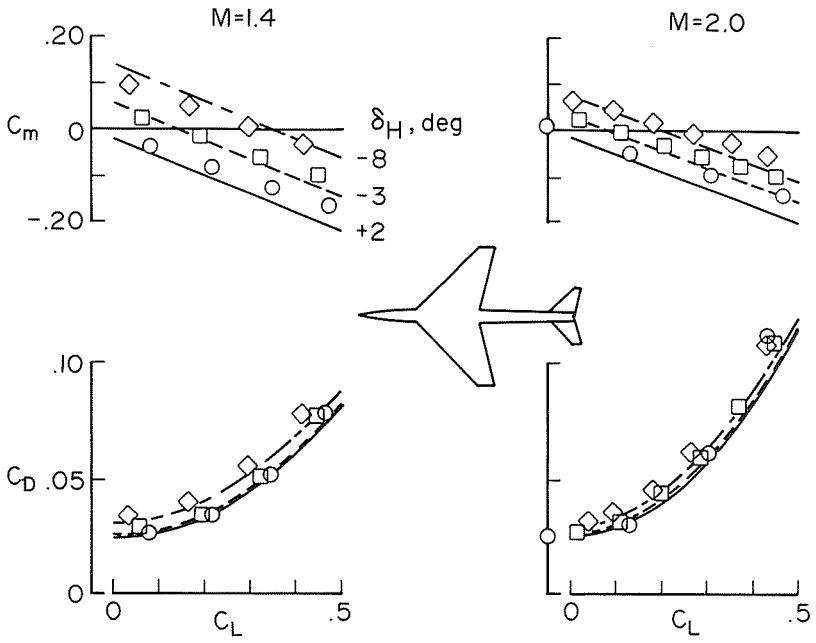

Figure 7. Arrow-wing configuration with horizontal tail.

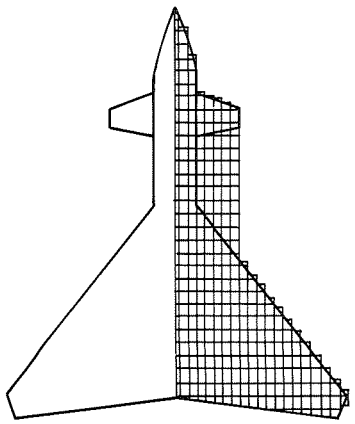

- CAMBERED AND TWISTED WING
- CAMBERED FOREBODY
- ARBITRARY PLANFORM WING
- ARBITRARY PLANFORM CANARD
- SLAB CANARD DEFLECTION

Figure 8. Canard-wing configuration.

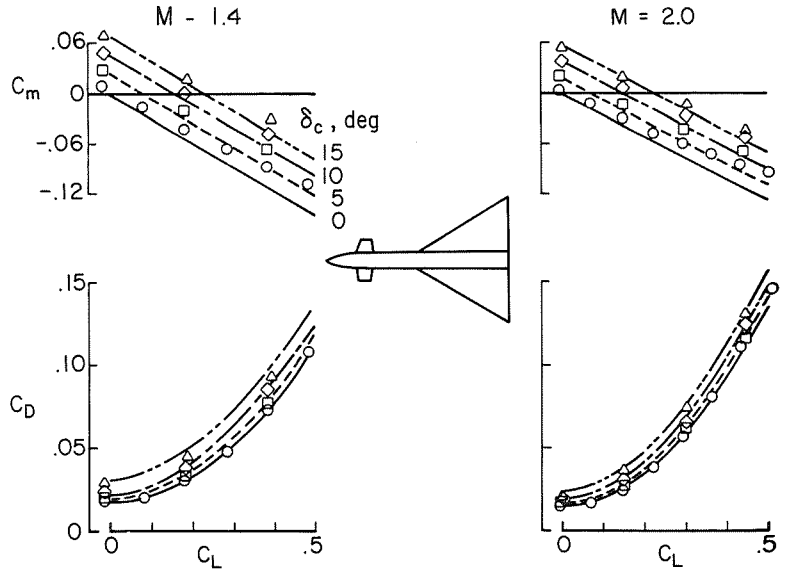

Figure 9. Delta-wing configuration with canard.

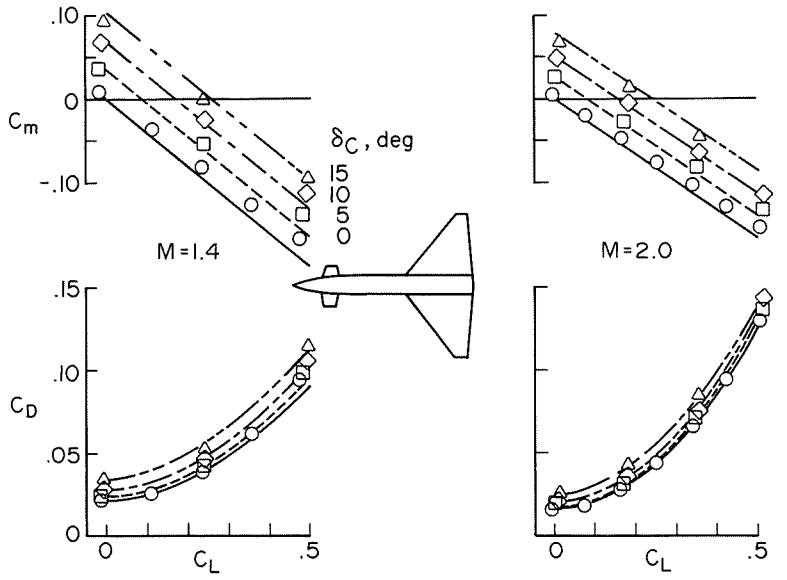

Figure 10. Trapezoidal-wing configuration with canard.

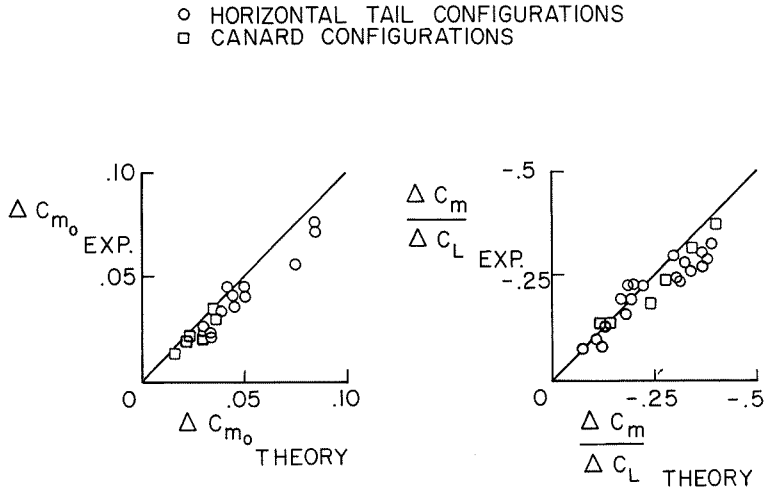

Figure 11. Theoretical and experimental stability and control parameters.

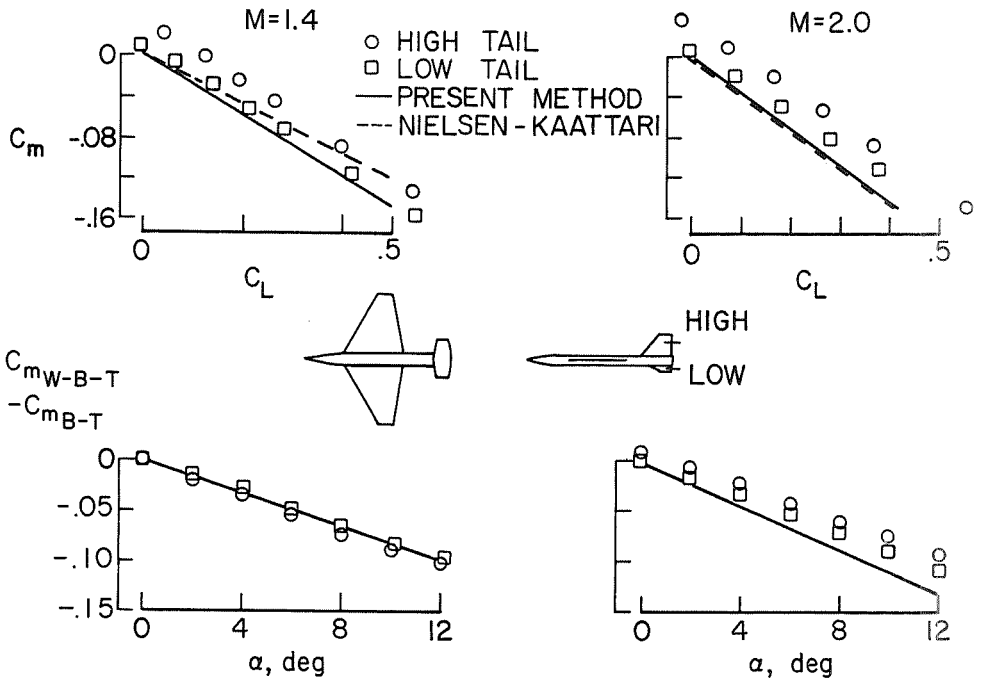

Figure 12. Effect of vertical location of horizontal tail.

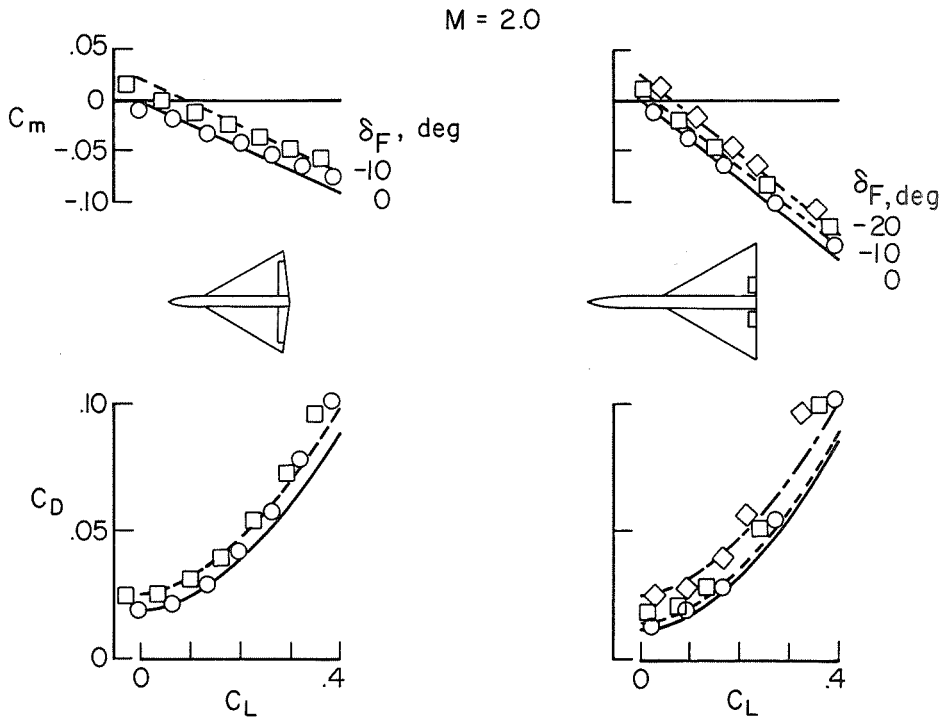

Figure 13. Configurations with trailing-edge controls.